Adv. Polar Upper Atmos. Res., **14**, 76–92, 2000

Conjugate features of daytime absorption associated with specific changes in the solar wind observed by inter-hemispheric high-latitude imaging riometers

Masanori Nishino[1], Hisao Yamagishi[2], Natsuo Sato[2], Ruiyuan Liu[3], Hongquao Hu[4], Peter Stauning[5] and Jan A. Holtet[6]

[1]*Solar-Terrestrial Environment Laboratory, Nagoya University, Honohara, Toyokawa 442-8507*
[2]*National Institute of Polar Research, Itabashi-ku, Tokyo, 173-8515*
[3]*Polar Research Institute of China, Shanghai, 200129, China*
[4]*Wuhan University, Wuhan 430072, China*
[5]*Danish Meteorological Institute, Copenhagen, Denmark*
[6]*The University of Oslo, Oslo, Norway*

Abstract: Imaging riometers at Ny-Ålesund (NYA) and Danmarkshavn (DMH) in the Arctic and Zhongshan (ZHS) in Antarctica were used to examine conjugate features of daytime ionospheric absorption in the polar cusp/cleft for specific changes in solar wind plasma parameters and the interplanetary magnetic field (IMF). We observed absorption spikes in the afternoon (1300–1500 MLT) associated with a steep increase in the high solar wind dynamic pressure and a synchronized spike-type IMF excursion. Afternoon absorption was identified between the stations at NYA and ZHS. The absorption extended longitudinally over a few hundred km, in a narrow arc about 50 km wide in latitude. Magnetic field compression associated with the steep pressure increase may stimulate substorm electrons drifting eastward from the nightside magnetosphere through the inner edge of the LLBL. We also observed absorption spikes around noon that were associated with a sudden pressure increase and a synchronized IMF excursion after a prolonged quiet state. The noon absorption was identified simultaneously at the DMH and ZHS inter-hemispheric stations. It extended longitudinally for several hundred km, including a small gap of about 50 km, and for over 400 km wide in latitude. Magnetic field compression associated with the sudden pressure increase may stimulate a population of magnetospheric electrons located at the equatorward boundary of the cusp/cleft.

1. Introduction

Symmetric and asymmetric configurations of the magnetosphere between sunlit and dark ionosphere conditions have been studied using concurrent riometer observations at high latitudes in Longyearbyen (74.4°N geomag. lat.) in Svalbard and at Mirny (77.0°S geomag. lat.) in Antarctica using a conventional 30 MHz broad-beam riometer (Eriksen *et al.*, 1964). Some cosmic noise absorption (CNA) events were observed from both the northern and southern hemisphere stations, while others were noted at stations in one hemisphere only. Conjugate riometer observations made from Frobisher Bay (L=15.0) in Canada and the South Pole (L=13.3) have demonstrated that conjugate CNA events tend

to occur with greater intensity in the local winter, and there are significant time differences in their maximum intensities (Hargreaves and Chivers, 1965). In addition, using conjugate riometer observations at Frobisher Bay and the South Pole, Rosenberg (1987) found that ionospheric absorption and intense electrojet currents in the dark ionosphere occurred preferentially in one hemisphere. He suggested that this was evidence of non-conjugate electron precipitation or severe distortion of the magnetic field-line topology in the nighttime sector. The conjugate features described above were for nighttime CNA events associated with substorms.

An imaging riometer for ionospheric study (IRIS), which is able to measure the spatial scale, shape, and movement of an absorption feature, was initially deployed at the South Pole (Detrick and Rosenberg, 1990). Nishino *et al.* (1998) demonstrated conjugate features of nighttime absorption events using IRIS instruments at hemispheric polar-cap stations: Ny-Ålesund (76.1°N geomag. lat.) and Longyearbyen (74.4°N) in Svalbard and Zhongshan (74.5°S) in Antarctica. They revealed that nighttime substorm absorption occurred simultaneously at stations in both hemispheres during strong geomagnetic disturbances, but the absorption structure differed between the stations when the east-west component (B_y) of the interplanetary magnetic field (IMF) was directed westward.

Recently, interest in the daytime ionospheric absorption in the polar cusp/cleft in studies of the solar wind-magnetosphere interaction at the dayside magnetopause has increased. Using the IRIS at Sondrestrom Fjord (73.7° invariant lat.) in Greenland, Stauning *et al.* (1995) and Stauning (1995) demonstrated that the poleward progression of the noon absorption was controlled by variation in the east-west IMF component (B_y) with a southward IMF (B_z<0). They interpreted the noon absorption feature as ionospheric *E*-region electron heating due to intensified electric fields in the open magnetic field-lines near the cusp poleward boundary associated with dayside magnetic reconnection. Using the four IRIS instruments in the European Arctic, Nishino *et al.* (1997) demonstrated another absorption feature near magnetic noon: this was a small-scale feature (100–200 km) superimposed on a large-scale extension of at least 700 km in longitude. This daytime absorption was interpreted in terms of variable precipitation of high-energy substorm electrons on closed magnetic field-lines drifting eastward from the nightside magnetosphere. To determine the mechanisms of the daytime absorption features and to understand the electrodynamics in the dayside magnetosphere, it is important to investigate conjugate absorption features in the polar cusp/cleft.

This paper is the first report of conjugate features of daytime absorption events in the polar cusp/cleft. In particular, we investigated the conjugate features of the daytime absorption events associated with specific changes in solar wind conditions when the dayside magnetosphere is strongly disturbed. In addition to the IRIS data from Ny-Ålesund and Zhongshan (Nishino *et al.*, 1998), IRIS data acquired at Danmarkshavn (77.3°N) on the east coast of Greenland are used. This paper presents daytime absorption events for two days along with simultaneous data for solar wind plasma parameters and IMF from the WIND satellite.

2. Conjugate observations

Table 1 shows the geographical coordinates of Danmarkshavn (DMH), Ny-Ålesund

Table 1. Geographical coordinates of Danmarkshavn (DMH), Ny-Ålesund (NYA), and Zhongshan (ZHS) and their corrected geomagnetic latitude, approximate magnetic noon, and total magnetic field according to the IGRF model.

Stations	Geographical coordinates	Corrected geomag. latitude	Eccentric dipole magnetic noon	Total magnetic field
Danmarkshavn (DMH)	76.77N 18.66W	77.26	1036 UT	53660 nT
Ny-Ålesund (NYA)	78.92N 11.92E	76.05	0847 UT	53959 nT
Zhongshan (ZHS)	69.37S 76.38E	−74.52	1014 UT	53733 nT

(NYA), and Zhongshan (ZHS) and their corrected geomagnetic latitudes, eccentric dipole magnetic noon, and the total intensity of the magnetic field according to the IGRF model.

The IRIS instruments at ZHS and DMH have almost the same antenna configurations, two-dimensional 8 by 8 dipole-elements with a half-wavelength spacing at 38.2 MHz, while the instrument at NYA has two-dimensional 8 by 8 dipole-elements with a 0.65 wavelength spacing at 30 MHz. Figure 1 shows the projection of the half-power width patterns of the 64 antenna beams at an ionospheric absorption altitude of 90 km. The patterns are shown for (a) half-wavelength spacing and (b) 0.65-wavelength one (Yamagishi *et al.*, 1992). The IRIS fields-of-view (FOV) are squares that contain most of the antenna beams and have sides of approximately 400 km and 200 km for DMH/ZHS and NYA, respectively. The 8 by 8 beams formed are called N1, N2, ... N8, or S1, S2, ... S8 in the north-south cross section, and as E1, E2, ... E8 in the east-west one. Note that beams S1-S4 at ZHS are directed towards high latitudes. The technical details of the IRIS instruments and the reduction process used for the absorption data have been reported by Stauning *et al.* (1992), Nishino *et al.* (1998), and Nishino *et al.* (1993) for the DMH, ZHS, and NYA stations, respectively.

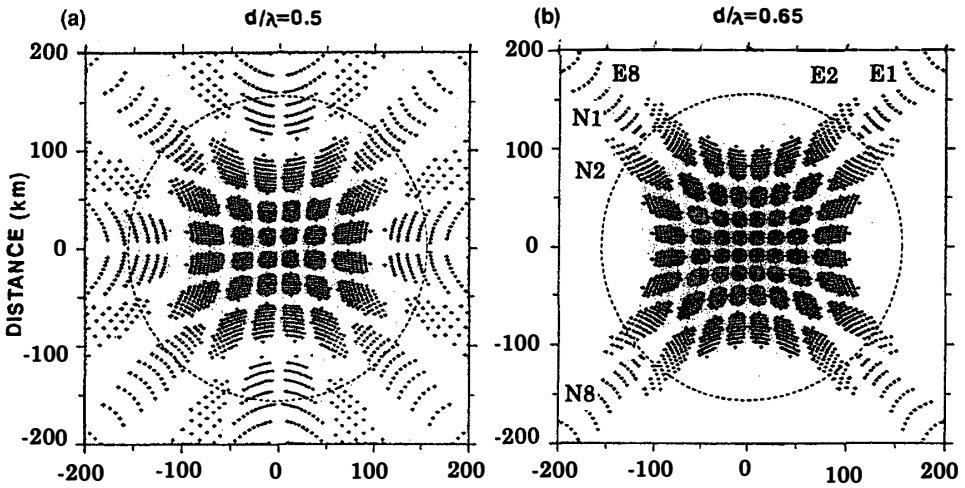

Fig. 1. The projection of a half-power width of the 64 antenna-beams onto an ionospheric absorption altitude of 90 km. The patterns are shown for (a) 0.5-wavelength spacing (Zhongshan station) and (b) 0.65-wavelength spacing (Ny-Ålesund station) (after Yamagishi et al., 1992). The beam numbers are assigned for north-south and east-west cross sections in pattern (b).

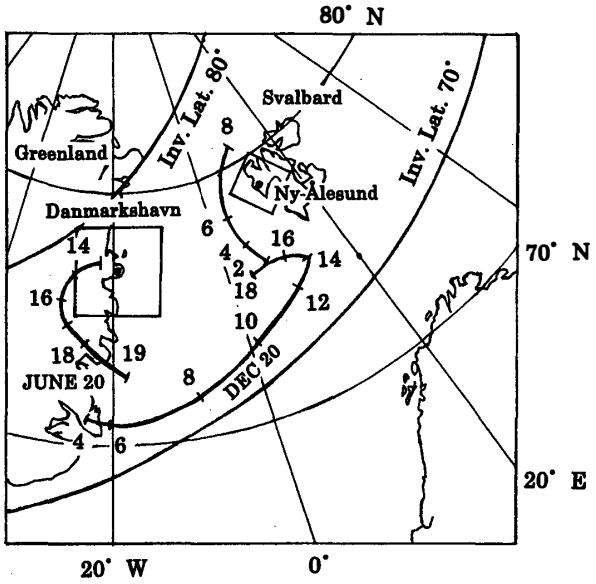

Fig. 2. The IRIS FOV at Danmarkshavn and Ny-Ålesund with the invariant latitudes on a map of the European arctic. Daily variation in the conjugate points for Zhongshan is drawn for the northern summer and winter solstices, based on calculations using the 1996 Tsyganenko model (modified after Yamagishi et al., 1998).

Figure 2 shows the locations of DMH and NYA on a map of the European Arctic with the approximate field-of-view (FOV) of each IRIS with invariant latitudes of 70°N and 80°N. The north-south axes of the DMH-, NYA-, and ZHS-FOV are directed towards geomagnetic north, the approximate eccentric magnetic dipole, and geomagnetic south, respectively. Daily variation in the conjugate points of ZHS calculated using the 1996 Tsyganenko model (Tsyganenko and Stern, 1996) for the IMF conditions $B_y = B_z = 0$ is displayed for UT for the northern summer (June 20) and winter (Dec. 20) solstices (Yamagishi *et al.*, 1998).

2.1. The daytime absorption event on August 3, 1997

The upper panel of Fig. 3 shows variation in the B_x, B_y, and B_z components of the IMF, ion density, and ion dynamic pressure of the solar wind observed from the WIND satellite during 1030-1400 UT on August 3, 1997, while the lower panel shows variation in the absorption of the east-west beams near the zenith (S4) at ZHS during 1100–1330 UT. During this period, the satellite was located at R_x~+80 R_e, R_y~–60 R_e, and R_z~+15 R_e (in GSE). The solar wind dynamic pressure increased from a quiet state (~2 nPa) to ~6 nPa at 1005 UT, remained at 6–8 nPa, and decreased to 6 nPa at about 1100 UT. Subsequently, the pressure showed a positive swing (~8 nPa) at about 1132 UT, a gradual step-like increase at about 1150 UT, and a steep increase at about 1200 UT, followed by a quasi-periodic oscillation until 1305 UT. Between 1100–1300 UT, IMF B_x was almost positive, and IMF B_y was positive with a gradual negative change at about 1230 UT. IMF B_z gradually changed from negative to positive with a sharp negative spike (~2 nT) around 1200 UT. To show the relationship between the solar wind conditions and absorption features, we use a total time delay of 20 min to account for propagation from the satellite to the magnetopause at an average solar wind velocity of

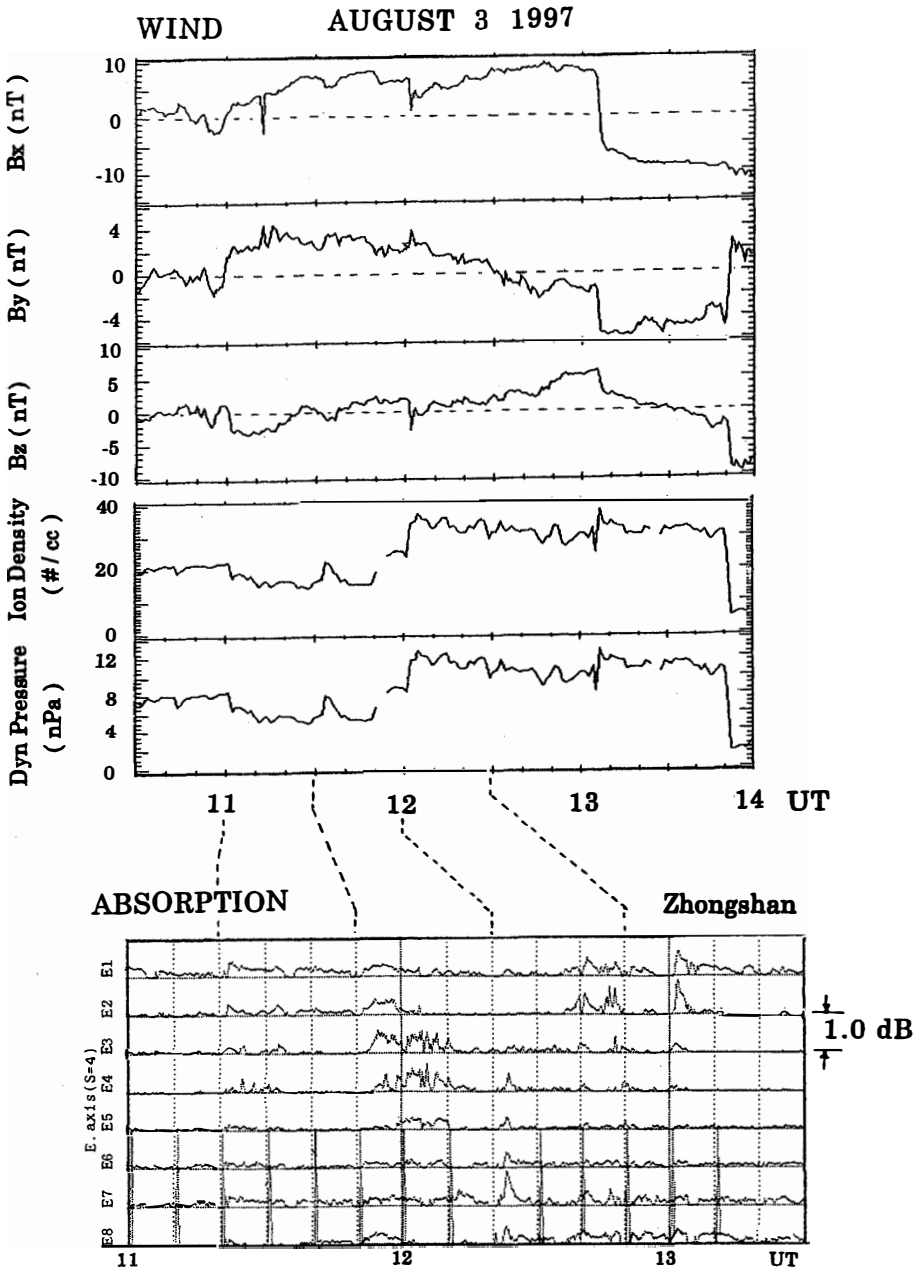

Fig. 3. Variation in the B_x, B_y, and B_z components of the IMF, ion density, and ion dynamic pressure of the solar wind determined from the WIND satellite during 1030–1400 UT on August 3, 1997 (upper panel). Variation in the ionospheric absorption in the east-west beams near the zenith during 1100–1330 UT at ZHS (lower panel). The dashed lines between the upper and lower panels show the 20-min delay.

400 km/s and from the magnetopause to the polar ionosphere (Stauning *et al.*, 1995). The dashed lines between the upper (WIND) and lower (absorption) panels show the 20-min delay.

Unfortunately, strong, impulsive radio waves transmitted every 10 min from the adjacent Digital Ionosonde during this period contaminated the cosmic radio signals near the western most beam (E8). Since magnetic noon is 1014 UT at ZHS (see Table 1), the

absorption occurred in the afternoon (1300–1500 MLT). Here, we focus on the absorption feature associated with the increases in solar wind dynamic pressure at around 1133, 1150, and 1200 UT. The absorption spikes seen in the eastern beams (E1–E4) around 1153 UT likely correspond to the positive swing in the pressure and the small negative dip in IMF B_z at about 1135 UT. The subsequent fluctuating spikes (E3 and E4)

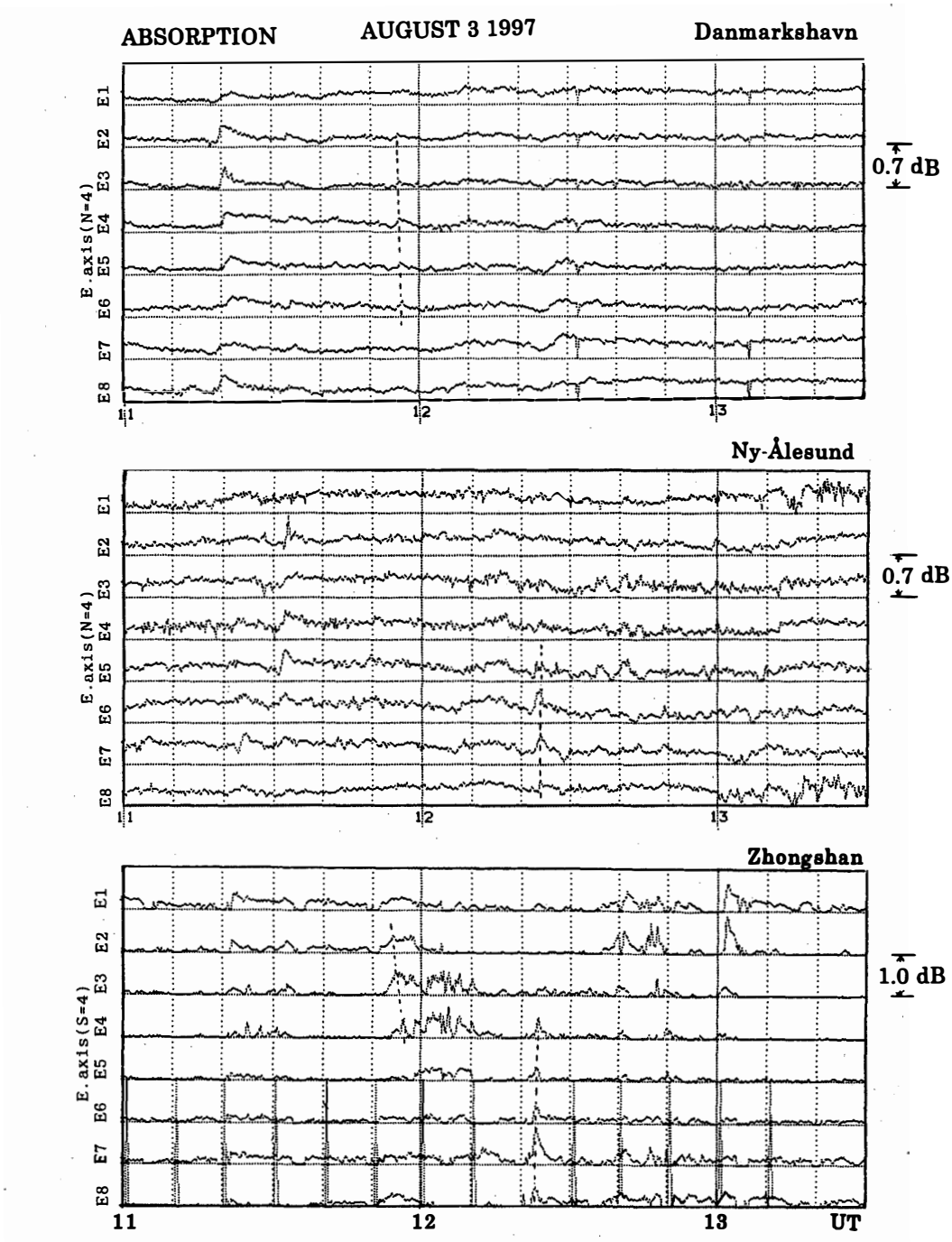

Fig. 4. Variations in the absorption at DMH, NYA, and ZHS during 1100–1330 UT on August 3, 1997. The variation is displayed for the east-west cross sections near the zenith beam for the three stations. The absorption unit is displayed to the right of the absorption data.

from 1200–1210 UT seem to be false absorption. The absorption spikes seen only in beam E7 from 1210–1216 UT may correspond to the gradual step-like increase in the dynamic pressure around 1150 UT. It should be noted that the pronounced absorption spikes seen in the east-west beams at 1223 UT clearly correspond to the steep pressure increase and the synchronous spike-type changes of the IMF components around 1200 UT. The succeeding quasi-periodic absorption spikes, seen best on beam E7, seem related to pressure oscillation after the steep increase.

Figure 4 shows time variation in the absorption in the east-west beams near the zenith at DMH, NYA, and ZHS during 1100–1330 UT. The intensities of the absorption spikes are mostly below 1 dB at all three stations. However, it is evident that the absorption intensity in the southern hemisphere is larger than that in the northern hemisphere, indicating asymmetry due to the sunlit and dark ionosphere (Eriksen *et al.*, 1964). The absorption spikes at ZHS around 1154 UT likely correspond to the very weak absorption (<0.2 dB) seen in beams E2–E6 at DMH (shown by dotted lines). The absorption spikes seen only in beam E7 at ZHS from 1212–1216 UT match the gradual and weak absorption features in beams E2–E6 at NYA, but it is unclear whether the absorption spikes at ZHS and NYA are identical. It is evident that the most pronounced absorption spikes seen around 1223 UT are identical at ZHS and NYA (shown by dotted lines). Thereafter, the absorption spikes seen in beams E1–E3 at ZHS around 1240 UT are likely identical with those in beams E1–E5 at NYA.

In order to investigate conjugate features of the pronounced spikes at 1223 UT in detail, we show the variation in the absorption spikes in both the north-south and east-west cross sections at ZHS (left side) and NYA (right side) with time in Fig. 5. The absorption spikes at ZHS in the Southern Hemisphere extend over 200 km in an east-west direction, with the greatest enhancement approximately 100 km west of the zenith, while they are very narrow in the north-south direction, about 50 km wide. This arc-type absorption matches arc-type auroras observed simultaneously by the all-sky TV at ZHS in the southern winter (Y. Murata, private communication). On the other hand, the absorption spikes at NYA in the Northern Hemisphere are on a smaller scale, but similar in shape to those seen at ZHS. Figure 5 also shows that the arc-shape absorption shows southeastward motion at a velocity of about 3.7 km/s at ZHS, which corresponds to the geomagnetic eastward motion, and also shows a geomagnetic eastward motion of about 1.2 km/s at NYA in the Northern Hemisphere.

2.2. The daytime absorption event on November 22, 1997

The upper panel of Fig. 6 shows time variation in the B_x, B_y, and B_z components of the IMF, ion density, and ion dynamic pressure of the solar wind observed from the WIND satellite during 0800–1400 UT. The lower panel shows the variation in the absorption in the east-west beams (E1–E8) near the zenith at ZHS during 0900–1100 UT. As with the case for August 3, the absorption variation in beam E8 is contaminated by strong interference radio waves from the Digital Ionosonde. The satellite was located at R_x~+180 R_e, R_y~−17 R_e, and R_z~+28 R_e (in GSE). The solar wind dynamic pressure was steady at a small value (~2.5 nPa) before 0915 UT, and then suddenly increased to ~12 nPa and fluctuated. The IMF B_y component was steady and positive (~7 nT) until 0915 UT and a synchronized positive excursion with the sudden pressure increase was

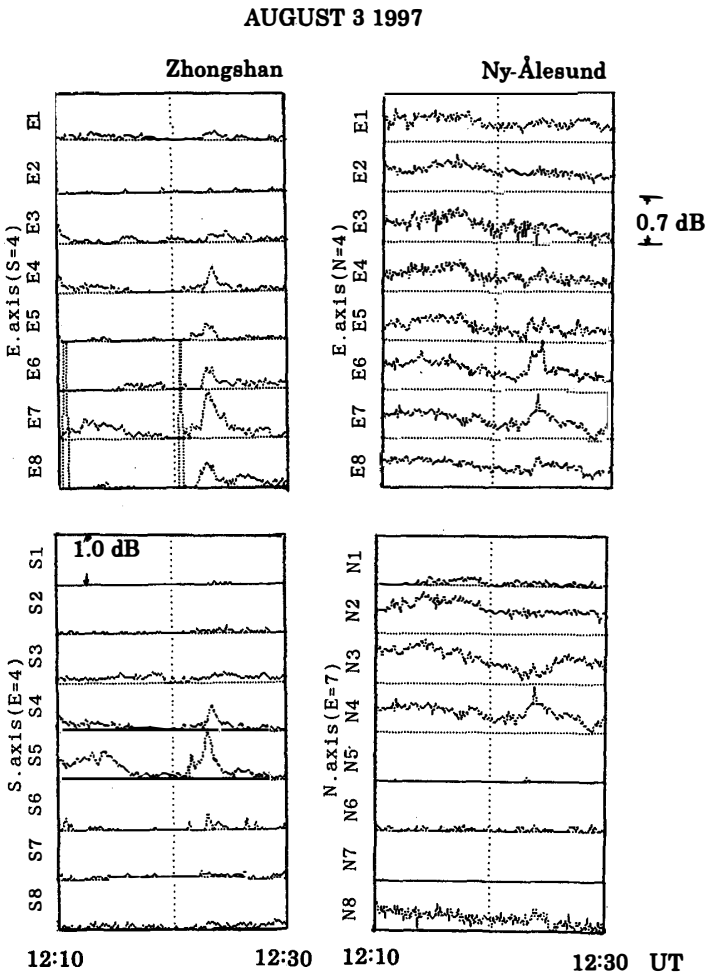

Fig. 5. Absorption at ZHS and NYA during 1220–1240 UT on August 3, 1997 using an expanded time scale. The variation is shown for east-west and north-south cross sections.

followed by fluctuations in positive amplitude until 12h UT. The IMF B_z component was also steady near zero until 0915 UT, when there was a synchronized positive excursion and a subsequent negative excursion followed by large positive and negative amplitudes. A delay time of 38 min accounts for the propagation from the satellite position to the magnetopause at an average solar wind velocity of 470 km/s and from the magnetopause to the polar ionosphere. Pronounced absorption spikes appeared at about 0952 UT with relatively strong intensity (~0.8 dB), indicating an association with the sudden increase in the solar wind dynamic pressure. The absorption occurred near magnetic noon. Thereafter, weak intensity (<0.3 dB) absorption recurred, as seen best on beam E4.

Figure 7 shows the variation in absorption between 0900–1100 UT at DMH, NYA, and ZHS. The variation is shown for the east-west beams near the zenith for NYA and ZHS, and in the southern part for DMH. The upper panel shows that the absorption intensity increases in all the beams at DMH around 0952 UT, and is greatly enhanced in the western beams (E7 and E8). In the middle panel, the absorption intensity increases in beams E5 and E8 at NYA around 0952 UT, but the absorption increase is not clear in the other beams. The absorption increase in beam E1 is false, due to the grating beam

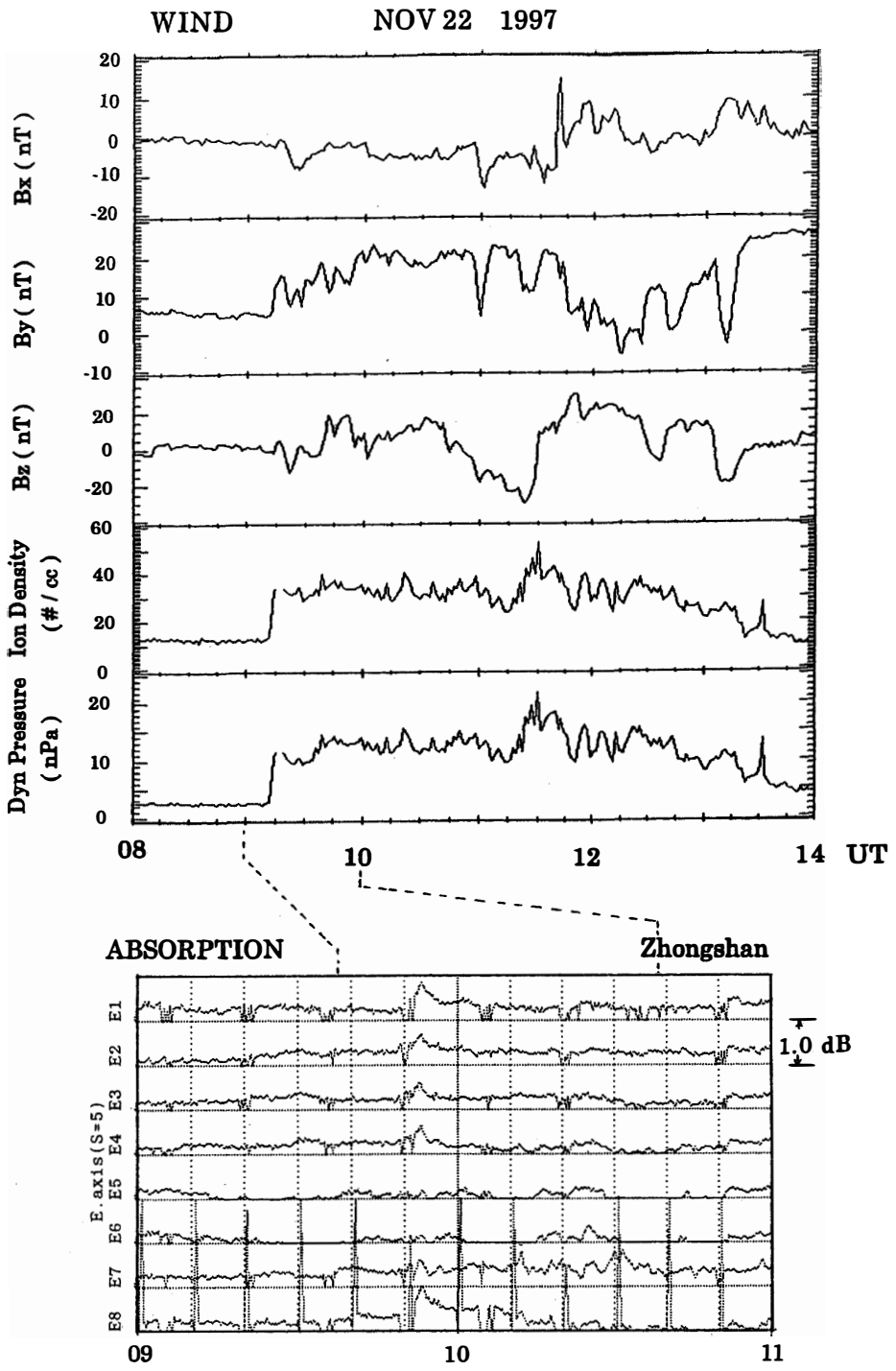

Fig. 6. Variation in the B_x, B_y, and B_z components of the IMF, ion density, and ion dynamic pressure of the solar wind determined from the WIND satellite during 0800–1400 UT on November 22, 1997 (upper panel). Variation in the ionospheric absorption in the east-west beams near the zenith during 0900–1100 UT at ZHS (lower panel). Dashed lines between the upper and lower panels show the 38-min delay.

produced outside beam E8 (Yamagishi *et al.*, 1992). Thus, it is estimated that the absorption region in the Northern Hemisphere extends from the western end of the NYA FOV to the western region outside the DMH FOV. The lower panel shows that the absorption intensity at ZHS around 0952 UT decreases in beams E5 and E6 compared

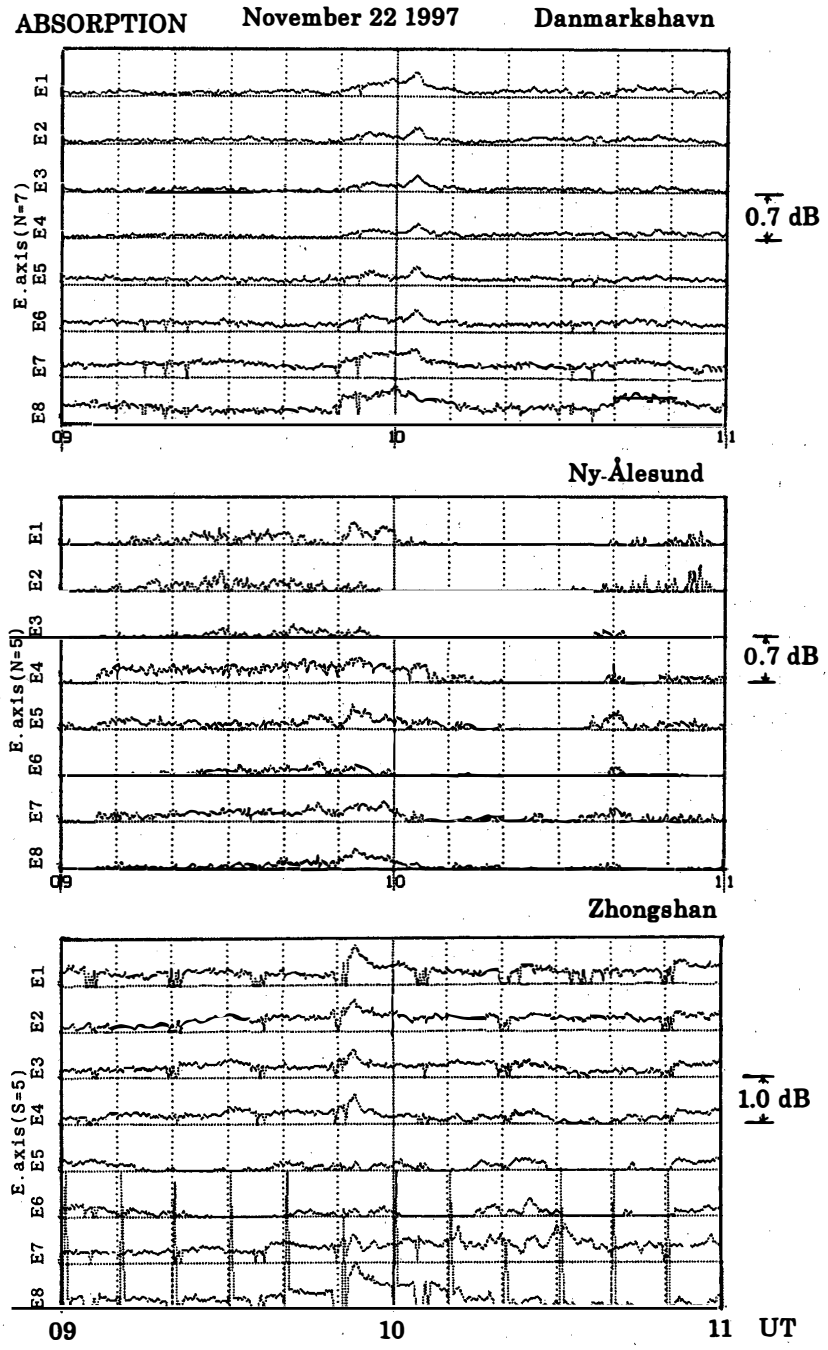

Fig. 7. Variation in the absorption at DMH, NYA, and ZHS during 0900–1100 UT on November 22, 1997. The variation is displayed for the east-west beams near the zenith at NYA and ZHS and in the southern part of the FOV for DMH. The absorption unit is displayed to the right of the absorption data.

with the intensities in the other eastern and western beams. That is, the absorption region extending over several hundred km in an east-west direction includes a small gap (50–100 km) near the zenith. Although we don't show the absorption variation in the north-south cross section at ZHS here, the absorption intensity is nearly equal in all the north-south beams at beam E4 near the zenith, indicating that the absorption region extends for more than 400 km in latitude. The succeeding absorption, which is enhanced in the eastern part of the DMH FOV at around 1004 UT, shows no corresponding absorption in the Southern Hemisphere.

3. Summary and discussion

In the previous section, we presented the conjugate features of daytime absorption events associated with specific changes in the solar wind dynamic pressure and IMF. This section summarizes the two absorption events, focusing on the absorption spikes associated with the steep and sudden increase in the solar wind dynamic pressure:

1) In the afternoon absorption event on August 3, absorption spikes are identified between the hemispherical stations, associated with a steep increase in the high solar wind pressure and synchronous changes in the IMF. The absorption region extends over a few hundred km in longitude, is approximately 50 km wide at the hemispheric stations, and shows eastward motion (anti-sunward).
2) In the noon absorption event on November 22, absorption spikes are identified between the hemispheric stations, associated with a sudden increase in the solar wind pressure and synchronized changes in the IMF after a prolonged quiet state. The absorption region extends for several hundred km in longitude, including a small gap, and is 400 km wide. The absorption shows no motion at either hemispheric station.

Early studies observed sudden commencement absorption (SCA) and sudden impulse absorption (SIA) at conjugate riometer stations in the auroral region (Leinbach *et al.*, 1970; Brown *et al.*, 1972). Observations of SCA and SIA at the South Pole (74.2° inv. lat.) revealed that these events were concentrated on the dayside of the magnetosphere (Brown, 1973). One SCA event observed at Godhavn (77.2° inv. lat.) occurred during quiet geomagnetic conditions during northward IMF (Brown, 1977). These observations were obtained using conventional broad-beam riometers; therefore, the spatial scale, structure, and movement of the absorption features were not reported.

First, this paper discusses the conjugate relationship between the hemispheric daytime absorption events.

3.1. Conjugate relationship

We show the daily variation of the conjugate points of ZHS on June 20 (northern summer) in Fig. 2. In the figure, the points are located in the western region far from Svalbard during 0200–0800 UT and around the east coast of Greenland during 1400–1900 UT. No conjugate points are obtained during 0800–1400 UT, around magnetic noon, or during 1900–0200 UT, around magnetic midnight, due to open magnetic field-line topology. As shown in Fig. 4, however, around 1223 UT on August 3, absorption spikes are observed between the stations at ZHS and NYA. The subsequent absorption spikes with a quasi-periodic feature also show a conjugate

relationship (correlation coefficient, 0.53). This indicates that a common driving mechanism operates in the closed magnetosphere, associated with specific changes in solar wind conditions.

From simple calculations of conjugate points using the T-96 model (Tsyganenko and Stern, 1996), we found that conjugate points in the afternoon sector tend to be displaced eastward by the pressure increase under quiet IMF conditions, while they are displaced westward by the positive IMF B_y under quiet pressure conditions. At 1156 UT, just before the steep pressure increase shown in Fig. 4, weak absorption is identified between stations ZHS and DMH (77.3° inv. lat.). At 1203 UT, the pressure increases steeply with a synchronized positive shift in IMF B_y, and the absorption is displaced south-eastward, nearer to station NYA (76.1° inv. lat.). It is predicted that the eastward displacement from DMH to NYA is preferentially due to the distortion of the magnetic field-line topology associated with the steep pressure increase.

From auroral observations at Ny-Ålesund, Sandholt *et al.* (1996) demonstrated that prenoon green line (557.7 nm) emissions that appeared in the southern part of the FOV shifted equatorward with a sudden increase in the solar wind dynamic pressure during the northward IMF. Newell and Meng (1994) produced a statistical map projecting magnetospheric regions into the ionosphere, based on precipitation characteristics under low (<2 nPa) and high (>4 nPa) solar wind conditions. In this map, the lower latitude boundary layer (LLBL) shifts to a lower-latitude region (75° MLAT) around 1200 MLT and is prolonged from ~0800 MLT to ~1600 MLT by high solar wind pressure, compared with the restricted time span under low pressure. On the other hand, Nishino *et al.* (1999) observed that the prenoon absorption at Ny-Ålesund was enhanced in the southern (low-latitude) part (~75° MLAT) of the FOV in association with the spike-type southward excursion of IMF B_z during persistent northward IMF. These IMF conditions are very similar to those encountered in our study. For the equatorward displacement of the present absorption, it is difficult to isolate the effects of the solar wind pressure from those of the IMF B_z orientation change.

It should be noted that the absorption spikes at 1156 UT show westward (sunward) motion, and those at 1223 UT show eastward (anti-sunward) motion associated with the steep pressure increase. This suggests that the absorption occurrence may be related to plasma flow changes in the cleft ionosphere. This inference will be discussed elsewhere, comparing to HF radar data in the polar region.

Concerning the noon absorption event on November 22, in Fig. 2 we show that conjugate points of ZHS are located near the geographic coordinate 74°N, 0°E at magnetic noon (~1000 UT) on the winter solstice (December 20). According to the T-96 model calculation, when the solar wind pressure suddenly increases from ~2.5 to 12 nPa, and the positive IMF B_y also increases to ~16 nT, the conjugate points would be displaced far to the southwest of DMH. In fact, the absorption was observed far to the southwest of DMH. However, since the absorption region extends over a wide range of longitude at stations in both hemispheres (see Fig. 7), it is difficult to evaluate the conjugate relationship exactly.

3.2. Source mechanism

Glassmier and Heppner (1992) suggested that pressure pulses of the solar wind at

the dayside magnetopause are a possible mechanism for transient geomagnetic field variation events on the ground. They further associated the compression of the magnetopause and the associated Alfven pulse with upward and downward field-aligned currents (FACs). Roeder and Lyons (1992) revealed that a distinct LLBL is nearly always identifiable in energetic particles measured between 1000–1400 MLT from satellite S3-3, and argued that the observed trapped pitch angle distributions of the energetic electrons imply that the LLBL is at least partially on closed magnetic field lines.

From ground optical observations, Farrugia *et al.* (1995) reported spontaneous enhancement of green auroral emissions (557.7 nm) of several kilo-Rayleighs around 1400 MLT at NYA associated with an increased solar wind dynamic pressure with IMF $B_z \sim 0$, $B_y \ll 0$. Such discrete auroral forms are considered the result of electron acceleration above the ionosphere, and auroral forms that have a limited east-west extent of a few hundred km may map to the inner edge of the LLBL or the LLBL/PS boundary. Sandholt *et al.* (1996) observed strong green line emissions at Ny-Ålesund in the hour before noon, which were associated with a steep increase in the solar wind dynamic pressure while IMF $B_y<0$. They revealed that the transient form at the equatorward boundary of the preexisting aurora might be explained by the generation of strong, localized FACs at the inner edge of the LLBL.

From ground IRIS observations at Sondre Stromfjord (73.7° inv. lat.), Stauning and Rosenberg (1996) proposed that the daytime absorption spikes, typically 0.2–0.3 dB, are related to the sudden precipitation of high-energy (30–300 keV) magnetospheric electrons, and are generated at or a few degrees equatorward of the convection reversal boundary, due to upward region-1 FAC intensification in the afternoon convection cell. This proposed mechanism explains the daytime absorption spikes that we observed. However, they were unable to determine a definite relationship between the daytime absorption spikes and the solar wind conditions.

As we showed in the previous section, the simultaneous arc-shaped auroras observed on August 3 at ZHS evidently manifest precipitation of high energetic electrons (> several keV) from the dayside magnetosphere into the high-latitude ionosphere. There is further evidence from absorption events obtained by the CANOPUS riometer chain in the nighttime sector during the present daytime absorption events. At the Rankin Inlet station (73°N geomag. lat.), an absorption event (~1 dB) occurred around 1130 UT on August 3 (courtesy of G. Rostoker), indicating the injection of substorm electrons into the nightside magnetosphere and the subsequent eastward drift of energetic electrons. Thus the magnetic field compression at the magnetopause associated with the steep increase in the solar wind dynamic pressure probably stimulates energetic electrons drifting eastward in the closed magnetosphere, resulting in precipitation into the cleft ionosphere.

During the noon absorption event on November 22, the noon absorption spikes were associated with the sudden pressure increase after a prolonged, reduced solar wind dynamic pressure for the conditions $B_z \sim 0$ and $B_y>0$. The absorption region covers a wide east-west span, with a small gap near the zenith at ZHS. We again checked the Rankin Inlet riometer data for the occurrence of absorption events, and found a weak absorption event during the hour before 1000 UT.

Brown (1973) observed sudden impulse daytime absorption (SIA) events at the South Pole station after prolonged magnetic quiet. He suggested that an energetic electron population that developed earlier in the nearby boundary region might be precipitated into the polar cusp/cleft ionosphere. Thus magnetic field compression associated with the sudden increase of the solar wind pressure probably stimulates a population of magnetospheric electrons at the equatorward cusp boundary.

3.3. Quasi-periodic absorption feature

Farrugia *et al.* (1995) revealed that strong, impulsive changes in the solar wind dynamic pressure while IMF B_z~0 and B_y<0 stimulated the increase in auroral brightening in the cusp/cleft ionosphere. On the other hand, Sibeck *et al.* (1989) reported an oscillation in the riometer absorption with an 8–10 min period near magnetic noon at the South Pole (L=13.3). They interpreted this as magnetic field compression associated with a dynamic pressure oscillation of the solar wind propagated earthward as a compressed MHD wave, which simultaneously perturbed the quasi-periodic electron population in the dayside magnetosphere.

Figure 3 shows a quasi-periodic variation (period, 300–500 s) in the absorption feature on beam S4E7 at ZHS during 1220–1310 UT. We examined whether the periodic feature of this absorption is related to the pressure oscillation during 1200–1300 UT.

Figure 8 shows an enlarged display of the variation in the S4E7-absorption at ZHS (dotted line) and the N4E5-absorption at NYA (light solid line) during 1220–1310 UT, together with the variance of the pressure when it exceeded 9 nPa (heavy solid line) from 1200–1250 UT satellite time (1220–1310 UT on the ground). The correlation coefficients between the pressure oscillation and the S4E7 absorption (ZHS) and the pressure oscillation and the N4E5 absorption (NYA) are 0.50 and 0.35, respectively, taking only the absorption spikes exceeding 0.1 dB. These coefficients are not high enough to state definitely that the solar wind pressure oscillation is directly connected to the occurrence of the ionosphere absorption. For example, the gradual pressure increases

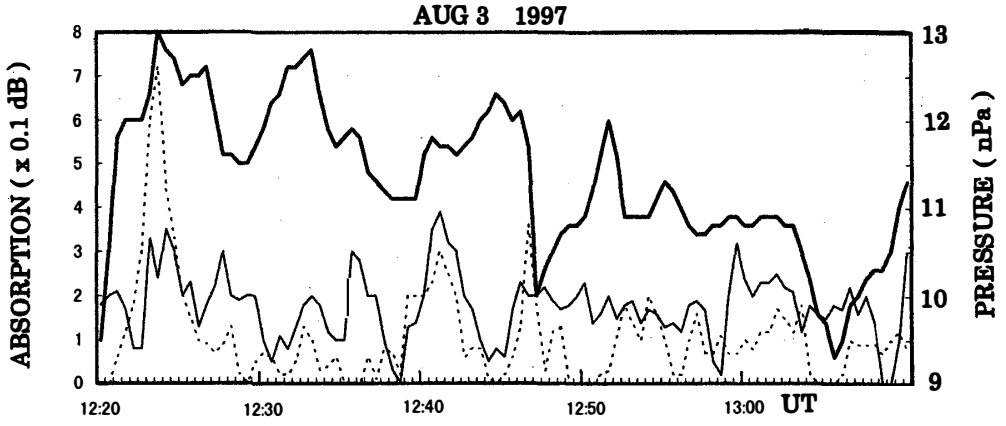

Fig. 8. Detailed variation in the absorption on the S4E7-beam (dotted line) at ZHS and on the N4E5-beam (light solid line) at NYA from 1220–1310 UT on August 3, 1997, together with the variance of the pressure exceeding 9 nPa (heavy solid line) during 1200–1250 UT satellite time.

between 1230–1235 UT and 1243–1248 UT do not contribute to the absorption occurrence. A pressure pulse in the solar wind at the dayside magnetopause might cause transient geomagnetic field variation on the ground (Glassmier and Heppner, 1992). We plan to investigate the ground geomagnetic variation in the polar cusp/cap obtained using the IMAGE magnetometer network (Lühr *et al.*, 1998).

4. Concluding remarks

We report two daytime absorption events observed using IRIS at the DMH/NYA and ZHS inter-hemispheric stations. This paper examines the conjugate features, focusing on the absorption events associated with the increased solar wind dynamic pressure. We came to the following conclusions in this case study:

1) Afternoon absorption spikes from 1300–1500 MLT associated with a steep increase in the high solar wind pressure were identified at inter-hemispheric stations between NYA and ZHS. The absorption extends over a few hundred km longitudinally in an arc with a narrow latitudinal width (~50 km) and shows eastward motion. Magnetic field compression associated with a pressure impulse may stimulate energetic electrons drifting eastward from the nightside magnetosphere through the inner edge of the LLBL. The quasi-periodic absorption feature shows no direct response to the oscillation of the solar wind dynamic pressure.
2) The noon absorption spikes from 1100–1300 MLT associated with the sudden increase after the prolonged quiet solar wind and IMF conditions are identified at the inter-hemispheric stations between DMH and ZHS. The absorption extends for several hundred km longitudinally, including a small gap (50–100 km), and is about 400 km wide. The magnetic field compression associated with a sudden pressure increase may stimulate a population of magnetospheric electrons near the cusp equatorward boundary.

Further analysis of the daytime absorption associated with specific changes in the solar wind dynamic pressure is required to determine the exact source mechanisms.

Acknowledgments

We would like to thank A. Egeland, University of Oslo, for arranging the riometer observations at Ny-Ålesund. We gratefully acknowledge the collaborating people operating imaging riometers at Ny-Ålesund and Zhongshan in the Norwegian Polar Institute and Chinese Antarctic Expedition Party, respectively. We also gratefully acknowledge Ron Lepping and K. Ogilvie, NASA Goddard Flight Center, for supplying the WIND satellite data and G. Rostoker (presently at STE Laboratory, Nagoya University) for supplying the riometer data for the CANOPUS network through CDA-Web services. We thank anonymous referees for their kind comments in evaluating the paper.

The editor thanks Drs. Ryoichi Fujii and George J. Sofko for their help in evaluating this paper.

References

Brown, R.R. (1973): Sudden commencement and sudden impulse absorption events at high latitudes. J. Geophys. Res., **78**, 5698–5702.

Brown, R.R. (1977): Sudden commencement absorption events at the edge of the polar cap. J. Geophys. Res., **82**, 2433–2435.

Brown, R.R., Leinbach, H., Akasofu, S-I., Driatsky, V.M. and Schmidt, R.J. (1972): Quadruple conjugate pair observations of the sudden commencement absorption event on June 17, 1965. J. Geophys. Res., **77**, 5602–5607.

Detrick, D. and Rosenberg, T.J. (1990): A phased-array radio wave imager for studies of cosmic noise absorption. Radio Sci., **25**, 325–338.

Eriksen, K.W., Gillmor, C.S. and Hargreaves, J.K. (1964): Some observations of short-duration cosmic noise absorption events in nearly conjugate regions at high magnetic latitude. J. Atoms. Terr. Phys., **26**, 77–90.

Farrugia, C.J., Sandholt, P.E., Cowley, S.W.H., Southwood, D.J., Egeland, A., Stauning, P., Lepping, R.P., Lazarus, A.J., Hansen, T. and Friis-Christensen, E. (1995): Reconnection-associated auroral activity stimulated by two types of upstream dynamic pressure variations, Interplanetary magnetic field B_z~0, $B_y \ll 0$ case. J. Geophys. Res., **100**, 21753–21772.

Glassmeier, K.H. and Heppner, C. (1992): Traveling magnetospheric convection twin vortices: Another case study, global characteristics, and a model. J. Geophys. Res., **97**, 3977–3992.

Hargreaves, J.K. and Chivers, H.J.A. (1965): A study of auroral absorption events at the South Pole, 2. Conjugate properties. J. Geophys. Res., **70**, 1093–1102.

Leinbach, H., Schmidt, R.J. and Brown, R.R. (1970): Conjugate observations of an electron precipitation event associated with the sudden commencement of the magnetic storm. J. Geophys. Res., **75**, 34, 7099–7104.

Lühr, H., Aylward, A., Bucher, S.C., Pajunpaa, K., Holmboe. T. and Zalewski, S.M. (1998): Westward moving dynamic substorm features observed with the IMAGE magnetometer network and the ground-based instruments. Ann. Geophys., **16**, 425–440.

Newell, P.T. and Meng, C.-I. (1994): Ionospheric projections of magnetospheric regions under low and high solar wind pressure conditions. J. Geophys. Res., **99**, 273–286.

Nishino, M., Tanaka, Y., Oguti, T., Yamagishi, Y. and Holtet, J.A. (1993): Initial observation results with imaging riometer at Ny-Ålesund (L=16). Proc. NIPR Symp. Upper Atmos. Phys., **6**, 47–61.

Nishino, M., Yamagishi, H., Stauning, P., Rosenberg, T.J. and Holtet, J.A. (1997): Location, spatial scale and motion of radio wave absorption in the cusp-latitude ionosphere observed by imaging riometers. J. Atmos. Solar-Terr. Phys., **59**, 903–924.

Nishino, M., Yamagishi, H., Sato, N., Sanoo, Y., Liu, Ruiyuan, Hu, Honquao and Stauning, P. (1998): Initial results of imaging riometer observations at polar cap conjugate stations. Proc. NIPR Symp. Upper Atmos. Phys., **12**, 58–72.

Nishino, M., Nishitani, N., Sato, N., Yamagishi, H., Lester, M. and Holtet, J.A. (1999): A rectified response of daytime radio wave absorption to southward and northward interplanetary magnetic field: A case study. Adv. Polar Upper Atmos. Res., **13**, 139–153.

Roeder, J.L. and Lyons, L.R. (1992): Energetic and magnetosheath energy particle signatures of the low-latitude boundary layer at low altitude near noon. J. Geophys. Res., **97**, 13817–13828.

Rosenberg, T.J. (1987): Cosmic noise absorption at South Pole and Frobisher Bay: Initial results. Mem. Natl Inst. Polar Res., Spec. Issue, **48**, 161–170.

Sandholt, P.E., Farrugia, C.J., Stauning, P., Cowley, S.W.H. and Hansen, T. (1996): Cusp/cleft auroral forms and activities in relation to ionospheric convection: Responses to specific changes in solar wind and interplanetary magnetic field conditions. J. Geophys. Res., **101**, 5003–5020.

Sibeck, D.G., Baumjohann, W., Elphic, R.C., Fairfield, D.H., Fennel, J.F., Gail, W.B, Lanzerotti, L.I., Lopez, R.E., Luehr, H., Lui, T.Y., Maclennan, C.G., McEntire, R.W., Potemra, T.A., Rosenberg, T.J. and Takahashi, K. (1989): The magnetospheric response to 8-minute period strong-amplitude upstream pressure variations. J. Geophys. Res., **94**, 2505–2519.

Stauning, P. (1995): Progressing IMF By-related polar ionospheric convection disturbances. J. Geomagn.

Geoelectr., **47**, 735–757, 1995.

Stauning, P. and Rosenberg, T.J. (1996): High-latitude daytime absorption spike events. J. Geophys. Res., **101**, 2377–2396.

Stauning, P., Henriksen, S. and Yamagishi, H. (1992): Imaging riometer installation in Danmarkshavn, Greenland. Danish Meteorological Institute, Technical Report 92-4, 1–25.

Stauning, P., Clauer, C.R., Rosenberg, T.J., Friis-Christensen, E. and Sitar, R. (1995): Observations of solar-wind-driven progression of interplanetary magnetic field B_y-related dayside ionospheric disturbances. J. Geophys. Res., **100**, 7567–7585.

Tyganenko, N.A. and Stern, D.P. (1996): Modeling the global magnetic field of the large-scale Birkeland current systems. J. Geophys. Res., **101**, 27187–27198.

Yamagishi, H., Nishino, M., Sato, M., Kato, Y., Kojima, M., Sato, N. and Kikuchi, T. (1992): Development of imaging riometers. Nankyoku Shiryô (Antarct. Rec.), **36**, 227–250 (in Japanese with English abstract).

Yamagishi, H., Fujita, Y., Sato, N., Stauning, P., Nishino, M. and Makita, K. (1998): Conjugate features of auroras observed by TV cameras and imaging riometers at auroral and polar cap conjugate-pair stations. Polar Cap Boundary Phenomena, ed. by J. Moen *et al.* Kluwer Academic Publishers., 289–300.

(Received November 1, 1999; Revised manuscript accepted May 9, 2000)